american physiological society

JNP JOURNAL OF NEUROPHYSIOLOGY

J Neurophysiol 125: 2219–2227, 2021.
First published May 5, 2021; doi:10.1152/jn.00110.2021

RAPID REPORT

Neural Circuits

Movement signaling in ventral pallidum and dopaminergic midbrain is gated by behavioral state in singing birds

Ruidong Chen,[1] Vikram Gadagkar,[1,2] Andrea C. Roeser,[1] Pavel A. Puzerey,[1] and Jesse H. Goldberg[1]

[1]*Department of Neurobiology and Behavior, Cornell University, Ithaca, New York and* [2]*Department of Neuroscience, Zuckerman Mind Brain Behavior Institute, Columbia University, New York, New York*

Abstract

Movement-related neuronal discharge in ventral tegmental area (VTA) and ventral pallidum (VP) is inconsistently observed across studies. One possibility is that some neurons are movement related and others are not. Another possibility is that the precise behavioral conditions matter—that a single neuron can be movement related under certain behavioral states but not others. We recorded single VTA and VP neurons in birds transitioning between singing and nonsinging states while monitoring body movement with microdrive-mounted accelerometers. Many VP and VTA neurons exhibited body movement-locked activity exclusively when the bird was not singing. During singing, VP and VTA neurons could switch off their tuning to body movement and become instead precisely time-locked to specific song syllables. These changes in neuronal tuning occurred rapidly at state boundaries. Our findings show that movement-related activity in limbic circuits can be gated by behavioral context.

NEW & NOTEWORTHY Neural signals in the limbic system have long been known to represent body movements as well as reward. Here, we show that single neurons dramatically change their tuning from movement to song timing when a bird starts to sing.

basal ganglia; dopamine; movement; songbird; ventral pallidum

INTRODUCTION

Reward-related signaling in ventral tegmental (VTA) and ventral pallidal (VP) regions is strongly state dependent. For example, when an animal is hungry, a food predicting cue can drive dopamine release. But when sated, the DA system may be unresponsive (1, 2). Activity of VTA and VP neurons is also strongly driven by movements unrelated to reward (3–6). It remains unknown how these nonreward, movement-related signals depend on what an animal is actually doing.

Zebra finches engage in "bouts" of singing on and off during a typical day. Both during and outside these singing bouts, finches exhibit brief movements such as orienting their head and hopping from perch to perch (7, 8). Recently, we and others discovered that VP and VTA neurons encode singing-related neural activity, including performance error signals important for song learning (9–13). These error signals functionally resembled reward prediction error signals observed in the limbic system (14). We also discovered neurons with precisely time-locked firing to specific syllables in VP (9).

Here, we investigate the movement-related firing properties of VP and VTA neurons and how they depend on whether birds are singing or not. In both VP and VTA, we discovered neurons that change their tuning from movement to song timing as birds transition from nonsinging to singing states, demonstrating a gating mechanism for movement representation in limbic circuits commonly associated with reward and performance evaluation.

MATERIALS AND METHODS

Subjects, Surgery, and Histology

Subjects were 71 male zebra finches 74–355 days old singing undirected song. A total of 61 of 71 birds and 269 of 288 neurons were new analyses of previously published datasets (9, 10). Animal care and experiments were approved by the Cornell Institutional Animal Care and Use Committee. All

Correspondence: J. H. Goldberg (jessehgoldberg@gmail.com).
Submitted 10 March 2021 / Revised 26 April 2021 / Accepted 2 May 2021

surgeries were performed with isoflurane anesthetization. Custom-made microdrives carrying an accelerometer (Analog Devices AD22301), linear actuator (Faulhaber 0206 series micromotor), and homemade electrode arrays (5 electrodes, 3–5 MOhms, microprobes.com) were implanted into VP and VTA. VP implants (35 birds) were targeted using coordinates (4.4–5.4A, 1.1–1.5L, 3.5 V, head angle 20 degrees). VTA implants (36 birds) were targeted using antidromic methods with stimulation in Area X (5.6 A, 1.5 L, 2.65 V, head angle 20 degrees). After each experiment, small electrolytic lesions (30 μA for 60 s) were made with one of the recording electrodes. Brains were then fixed, cut into 100-μm-thick sagittal sections for histological confirmation of stimulation electrode tracks and reference lesions.

Singing and Nonsinging States

We separately analyzed neural activity and movement patterns in singing and nonsinging states, and during transitions between these states, as previously described (15, 16). Bouts of singing was defined as consecutive syllables produced with gaps shorter than 300 ms. Nonsinging states were silent periods at least 300 ms away from syllables. In analysis of movement outside singing, only movements with onsets at least 300 ms away from song were included.

Quantification of Movement

An accelerometer (Analog Devices AD22301) was mounted on each microdrive to detect gross body movements as described previously (9, 10). Briefly, movement onsets and offsets were determined by threshold crossings of the band-passed, rectified accelerometer signal. We further quantify the amplitude of each movement as the area under the curve of this signal (Fig. 1*A*).

To assess the probability of movement near vocalizations, we computed the fraction of trials (period surrounding syllable onsets and bout on/offsets) in which movement onsets were detected in 10-ms bins for all vocalizations from each bird. To assess the significance of peaks in these probability functions, we compared the highest probability peak to 1,000 surrogate probability functions generated by randomly time-shifting movement onset relative to syllable onsets. Probability peaks exceeding the 95th percentile of surrogate probability maximum were considered significant. For plots in Fig. 1, *B–D*, we took the mean and standard error of mean values from all birds. Syllables at the beginning and end of each bout were excluded from this analysis. Each bird had 811 ± 32 syllables and 157 ± 17 bouts.

To select similar movements shared between singing and non-singing states, we computed the joint distribution of duration and amplitude for all detected movements from each neuron, and restricted subsequent analysis to those movements that are shared in both conditions. In each bin, we randomly selected N movements from either state where N is the smaller number of movements in each state. Neurons that had at least 10 movements from each state were included for analysis. We confirmed the selected movements are sufficiently similar by performing two-sample Kolmogorov–Smirnov tests on the selected duration and amplitude distributions for each neuron.

Analysis of Neural Activity

Neural signals were band-passed filtered (0.25–15 kHz) in homemade analog circuits and acquired at 40 kHz using custom Matlab software. Spike sorting was performed offline using custom Matlab software (courtesy Dmitriy Aronov). Firing rate histograms were constructed with 10-ms bins and smoothed with a 3-bin moving average.

To quantify movement locked neural response, we computed *Z*-scored firing rates aligned to movement onsets during singing and nonsinging states using a 600-ms window centered on movement onsets as the baseline for each condition, respectively. This was chosen to reflect differences in degree of modulation rather than baseline firing rate between singing and nonsinging conditions. Movement index was defined as the highest absolute Z score within 100 ms before or after movement onsets. To assess the significance of these movement-locked rate modulations, we compared the highest rate peak and lowest nadir in movement onset-aligned rate histogram to 1,000 surrogate rate histograms generated by randomly time-shifting spike trains. Rate peaks exceeding the 95th percentile of surrogate rate maximum and rate nadirs below the 5th percentile of surrogate rate minimum were considered significant.

To calculate the latencies and durations of movement responses, spiking activity within ±300 ms relative to movement onset was binned in a moving window of 10 ms with a step size of 5 ms. Each bin was tested against all the bins in the first 200 ms using a Z test. Response onset (latency) was defined as the first bin for which the next four consecutive bins were significantly different from the prior activity (Z test, $P < 0.05$); response offset was defined as the first bin after response onset for which the next two consecutive bins did not differ from the prior (Z test, $P > 0.05$). Response duration was the difference between the offset and the onset times.

To quantify movement-related responses at song state boundaries, we computed z-scored firing rates aligned to movement onsets using only movements either immediately before or after onsets and offsets of singing bouts. Those state-dependent neurons that had at least 10 trials of each transition type were included in this analysis. Significant response to state boundaries was assessed with bootstrap method as above, and the duration of significant responses were quantified using z-test as above (Fig. 4*F*).

Song Timing-Related Activity

Intermotif pairwise correlation coefficient (IMCC) was used to identify neurons that had highly time-locked firing to song motifs (timing neurons), as previously described (9). Neurons with at least 10 motifs of singing were included in this analysis. Motif aligned instantaneous firing rate (IFR) was time warped to the median duration of all motifs, mean-subtracted, and smoothed with a Gaussian kernel of 20 ms SD, resulting in r_i for each motif. IMCC was defined as the mean value of all pairwise CC between r_i as follows:

$$IMCC = \frac{1}{N_{pairs}} \sum_{j>i}^{N_{pairs}} CC_{ij}$$

$$CC_{ij} = \frac{r_i \cdot r_j}{\sqrt{r_i^2 r_j^2}}$$

To assess the significance of IMCC values, we compared the true IMCC value to 1,000 surrogate IMCC values generated by randomly time-shifting spike trains. IMCC values were considered significant if greater than the 95th percentile of the surrogate values.

Classification of Neurons

We classified VP and VTA neurons by their song- and movement-related activity as follows:

Error neurons (N = 50): VP and VTA neurons were classified as error responsive (error neurons in Fig. 2) from previous studies (9, 10). Briefly, birds received syllable-targeted distorted auditory feedback (DAF) on randomly interleaved renditions. We compared target aligned activity between distorted and undistorted renditions, and those neurons with significant difference in firing following DAF were labeled as error neurons. Song timing neurons (N = 11) exhibited extremely precise song-locked bursting activity, operationally defined as IMCC > 0.3. Other neurons (N = 227): neurons not classified as either song error or song timing neurons (Fig. 2). VTAother (N = 146): following Ref. 10, these refer to those VTA neurons that did not exhibit song error response.

Movement-locked neurons (N = 103) had significant activity extrema near detected movement onsets during nonsinging period. State-dependent neurons (N = 32) had significant movement response during nonsinging but not during singing. Song-locked neurons (N = 71) exhibited song-locked firing with significant IMCC (inclusive of the extremely precise "song timing" neurons).

RESULTS

Measuring Neural Activity and Movement as Birds Transition Into and Out of Singing States

To test if neural activity correlated with movement timing, we recorded movements with accelerometers attached to head-mounted microdrives (Fig. 1A). In the recording chamber, most movements were head movements associated with orienting and whole body movements during hops. These transient movements occurred during both singing and nonsinging periods in the day. Movements were more likely to occur right before onset of syllables (Fig. 1B, peak movement onset probability 35 ± 2 ms before syllable onset, significant in 42 of 71 birds, assessed using bootstrap, see METHODS), as previously reported (10). At the level of singing bouts, movement probability peaked right before a bout of singing (Fig. 1C, peak movement onset probability 38 ± 0.2 ms before bout onset, significant in 61 of 71 birds, bootstrap) and trended down after singing (Fig. 1D, not significant). During nonsinging periods, movements were longer on average and their durations had higher variance (mean duration 106 ± 6 ms during singing vs. 159 ± 17 ms during nonsinging, N = 42,418 movements during, 44,850 outside singing, Fig. 1E), consistent with movements being more stereotyped during singing (8). To control for these differences, we include only those movements that have similar duration and amplitude in subsequent analysis (N = 35,227 movements during singing and nonsinging conditions, Fig. 1E, see METHODS).

VP and VTA Neurons Encode Movement Timing

We recorded VP and VTA neurons as birds transitioned between singing and non-singing states (n = 142 VP neurons, n = 146 VTA neurons, n = 71 birds) (9, 10). Many VP and VTA neurons exhibited activity that was precisely time-locked to movements outside of singing (26 of 142 neurons in VP, 77 of 146 neurons in VTA; rate extrema against randomly time-shuffled data with $P < 0.05$, METHODS). Most neurons exhibited brief rate increases after movement onsets (latency to rate increase: 6.43 ± 3.8 ms, duration: 69.9 ± 3.1 ms, n = 91 of 103 movement-related neurons, Fig. 2C), but neurons could also exhibit phasic decreases before movements (n = 12 of 103 neurons).

During our recordings, we controlled perceived error with distorted auditory feedback (DAF) (17, 18). On randomly interleaved renditions of "target" syllables, a brief, 50-ms snippet of sound was played through speakers surrounding the bird. In previous studies, we found that some VTA and VP neurons discharged differently to distorted and undistorted song renditions (9, 10). A small subset of these "error" responsive neurons also exhibited movement-locked discharge (Fig. 2, C and D, n = 1 of 23 VTA; n = 4 of 27 VP error neurons were movement related, $P < 0.05$, bootstrap, see METHODS).

In a previous study, we identified VP "song timing" neurons with bursts that were extremely locked to subsyllabic elements with millisecond timescale precision [operationally defined as intermotif pairwise correlation coefficient (IMCC) of 0.3 or higher] (15, 19,20). Interestingly, we found precisely timed firing in VTA as well, though these neurons were relatively rare. VTA neurons that were not error responsive (termed VTAother in Ref. 10) could also exhibit highly song-locked discharge (n = 6 of 144 VTA neurons tested; 2 of 146 VTA neurons were recorded for less than 10 motifs and excluded from this analysis, see METHODS), reported here for the first time. Most of these song timing neurons were movement-locked outside of singing (Fig. 2, C and D, n = 4 of 6 in VTA; n = 3 of 5 in VP, $P < 0.05$, bootstrap, see METHODS).

Movement-Locked Activity Can Depend on Behavioral State

To test if movement responses changed during singing, we compared movement-related changes in firing rate between singing and nonsinging states. Many neurons that were movement-locked outside of singing (Fig. 2C) lost their tuning to similar movements during singing (Fig. 2D and Fig. 3, N = 32 of 103 neurons with significant movement response only during nonsinging states, N = 71 of 103 neurons with significant responses in both singing and nonsinging states). In particular, five of five movement-related error neurons and four of seven movement-related timing neurons lost their movement tuning during singing.

We wondered whether these state-dependent firing patterns could be attributed to differential distribution of movement types in singing versus nonsinging states. We plotted the distribution of movement duration and amplitude from individual neurons in Fig. 3, B and D and confirmed the movements were not systematically different in either duration or amplitude (two-sample Kolmogorov–Smirnov test, $P > 0.05$, METHODS). As a group, state-dependent neurons

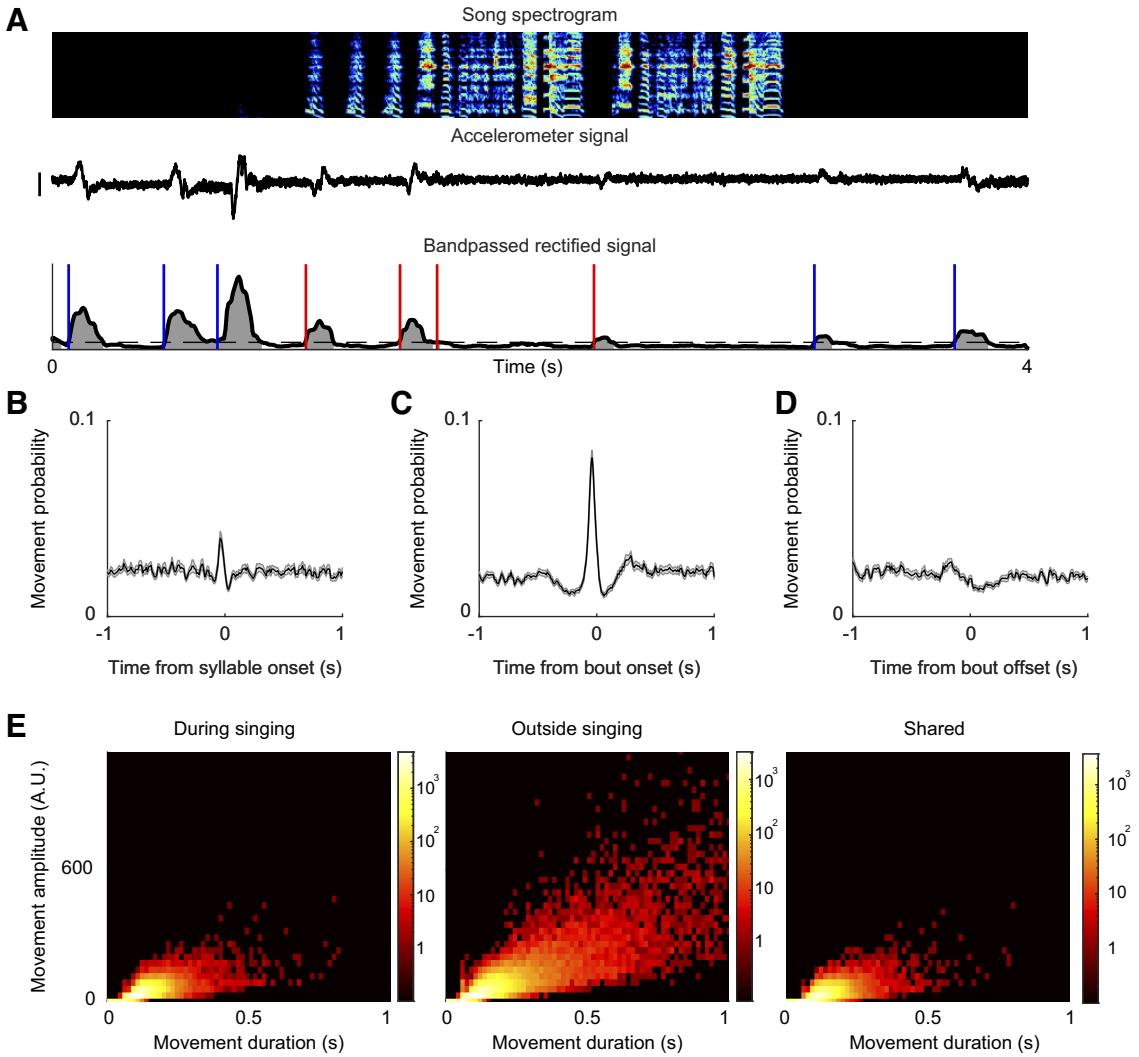

Figure 1. Measuring movement as birds transition into and out of singing states. *A*: (*top* to *bottom*) song spectrogram, accelerometer signal, and bandpassed rectified accelerometer signal. Blue lines indicate onset of movements outside singing, and red lines indicate onsets of movements during singing. Spectrogram frequency range: 500–7,500 Hz. Accelerometer signal scale bar: 0.05V. *B*: average probability of movement onsets around syllable onsets (mean ± SE, averaged from $N = 71$ birds). *C*: same as *B* for song bout onsets. *D*: same as *B* for song bout offsets. *E*: *left* and *middle*: distribution of duration and amplitude of movements during and outside singing for all birds ($n = 71$ birds, 42,398 movements in singing, 1,38,422 movements outside singing). Amplitude calculated as area under the curve of bandpassed rectified accelerometer signal (gray in *A*). Color axis: number of movements. *Right*: same axes as *left*, with data from shared movements between both conditions (35,227 movements from each condition). A.U., arbitrary units.

shared similar movement feature distribution as other neurons (31 of 32 state-dependent neurons had similar feature distributions, K–S test, $P > 0.05$). Mean ± variance of movement duration and amplitude for each state-dependent neuron shown in Fig. 3, *E* and *F*.

Movement-Related Neurons Switch to Song-Locked Firing during Singing

In both VP and VTA, movement-related neurons could be precisely time locked to song syllables during singing (Fig. 4, *A* and *B*, Ref. 9). Because song timing and movement timing are correlated during singing (cf. Fig. 1, *B* and *C*, and Ref. 10), a purely movement locked neuron could show spurious correlation to song timing. To test this, we compared the magnitude of movement aligned rate modulation between singing and nonsinging states. Movement modulation was quantified by the maximum in absolute value of *Z*-scored rate histogram, and song-locked firing was quantified by IMCC. Most neurons with significant time-locked firing to song showed higher movement selectivity outside singing than during singing ($n = 47$ of 71 neurons with significant IMCC, including 7 of 7 movement-related timing neurons, Fig. 4*C*). Conversely, most of the state-dependent neurons were song-locked ($n = 26$ of 32 state-dependent neurons had significant IMCC).

Movement Signaling Is Rapidly Gated at Transitions to Singing

To test if change in movement selectivity could occur immediately at state boundaries, we computed movement-aligned rate histograms for movements surrounding state transitions ($n = 53$ neurons with at least 10 transitions

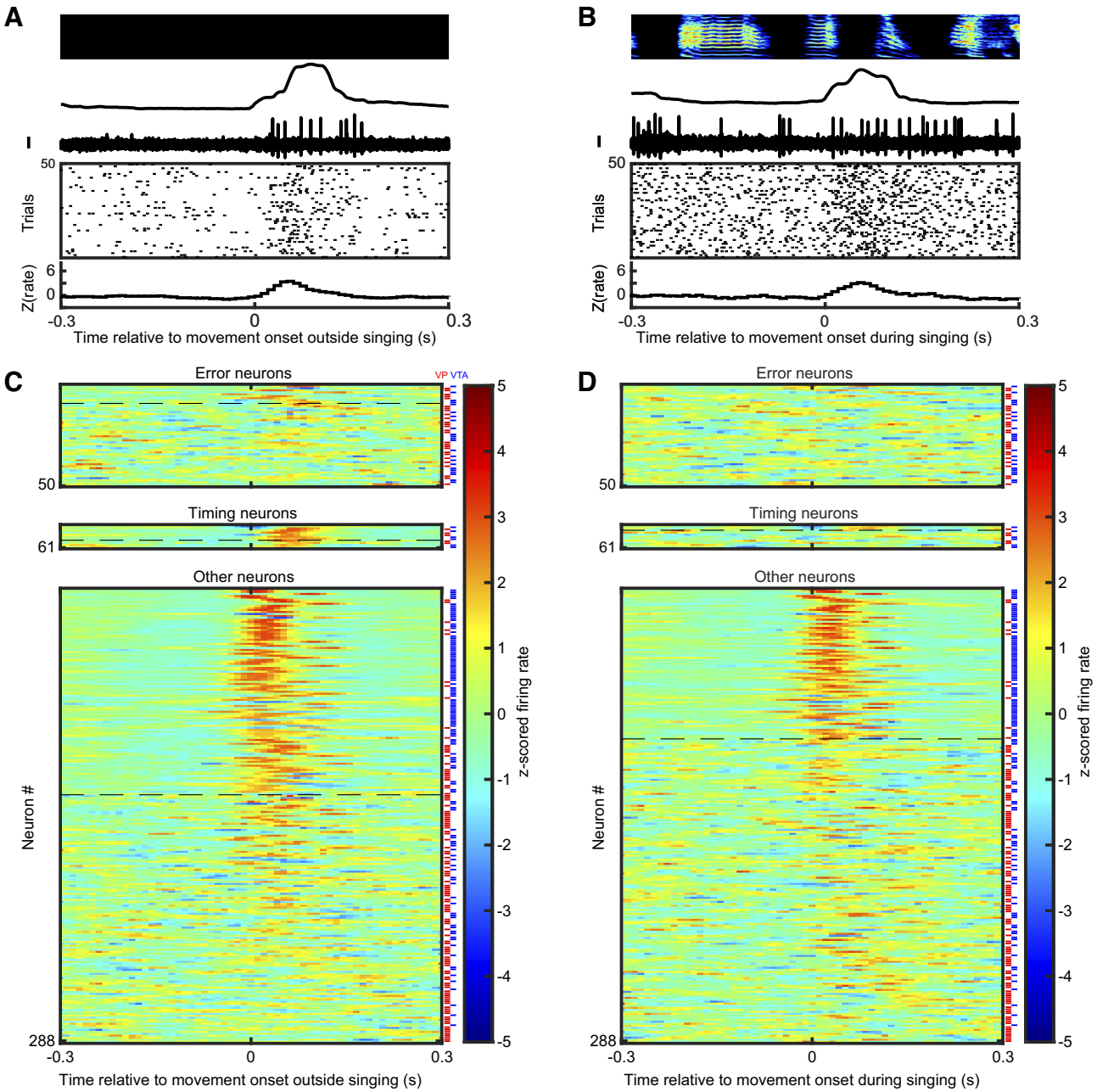

Figure 2. VP and VTA neurons exhibit movement-locked activity. *A*: example VP neuron recorded outside singing. *Top* to *bottom*: spectrogram, band-passed rectified accelerometer signal, neural voltage trace, raster plot of detected spikes, *Z*-scored firing rate. All plots are aligned to onsets of movements. Scale bar for neural activity is 0.25 mV. *B*: same neuron as in *A* but for movement onsets during singing. *C*: *Z*-scored firing rate aligned to movement onsets outside singing for all neurons, separated to error responsive, song timing related, and others. VP and VTA neurons are indicated by red and blue lines to the right of each row. Each group is separated into those with significant movement responses and those without by dashed horizontal lines, and sorted by maximum absolute response to movement onset. None of the error responsive neurons showed movement response during singing. *D*: same as *C* for movements during singing. Neurons are in the same order as in *C*. VP, ventral pallidum; VTA, ventral tegmental area.

tested). Whereas the last movements occurring immediately before song bouts were correlated with bursts of firing, the first movements within a song bout were not (Fig. 4, *D* and *F*, 493 transitions, 17 of 53 neurons tested, see METHODS). Similarly, movements immediately following bout offsets were reliably associated with a burst of activity even though similar movements during singing were not (Fig. 4, *E* and *F*, 647 transitions, 14 of 53 neurons tested). Thus, the change in tuning to movement can occur extremely rapidly (~0.1-s timescale) at transitions to and from singing state.

DISCUSSION

By recording neural firing during singing and nonsinging states in freely behaving birds, we discovered that movement-locked firing in VTA and VP neurons can be gated off

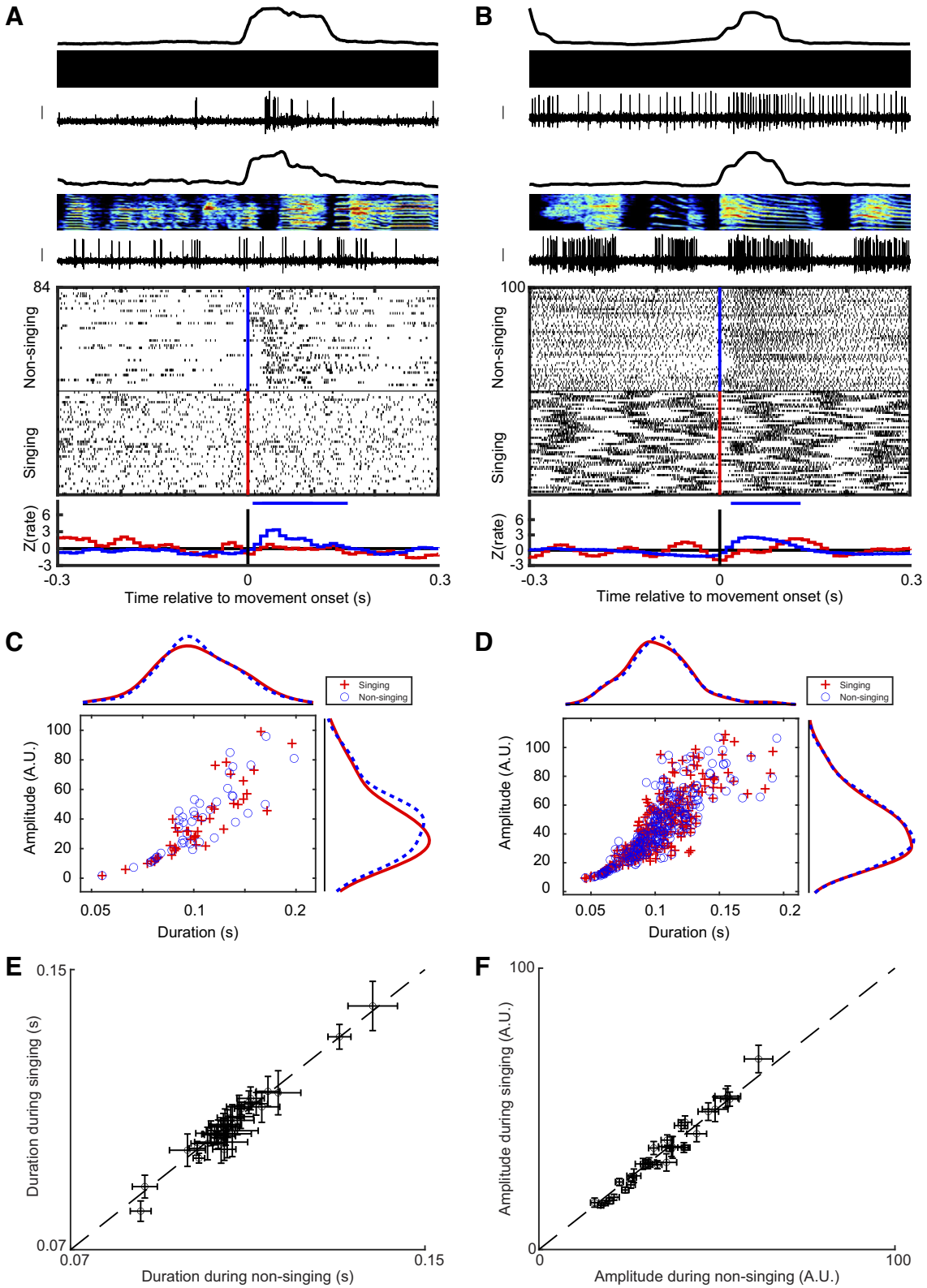

Figure 3. Example neurons that exhibit movement selectivity in the nonsinging state only. *A*: (*top* to *bottom*) bandpassed rectified accelerometer signal, spectrogram, voltage trace from an example VP neuron during nonsinging and singing states, raster plot of spiking activity, *Z*-scored firing rate histogram. Blue/red lines in the raster plot indicate movement onset during nonsinging/singing. Horizontal bars indicate the duration of significant response to movement (*Z* test, see METHODS). Scale bar for neural activity is 0.25 mV. *B*: same as *A* for an example VTA neuron. *C*: duration and amplitude of movements shown in *A* for singing (red pluses) and nonsinging (blue circles) states. Insets are kernel density plots of duration (*top*) and amplitude (*right*) of those movements. *D*: same as *C* for the neuron in *B*. *E*: duration of movements for state-dependent neurons. Circles are mean values from each neuron, error bars are SE. *F*: same as *E* for movement amplitude. A.U., arbitrary units; VP, ventral pallidum; VTA, ventral tegmental area.

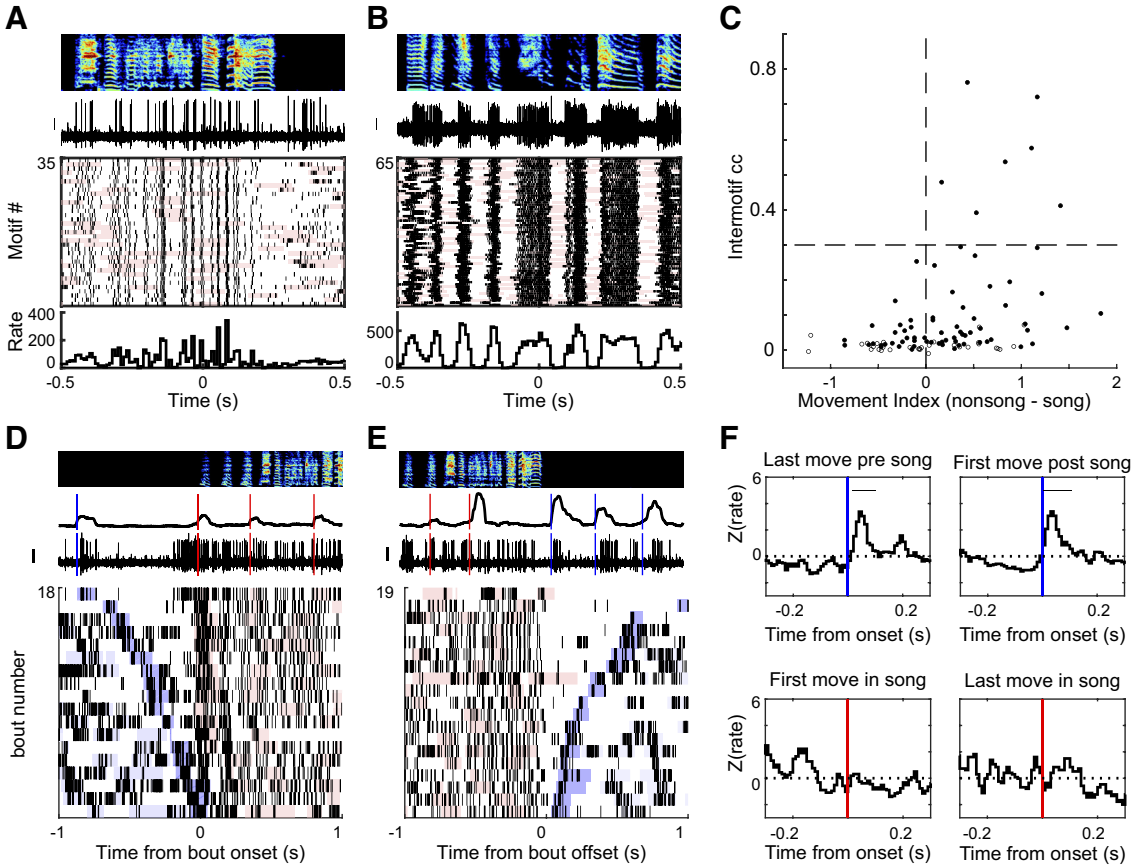

Figure 4. Example neurons that switch their tuning between song timing and movement at singing state boundaries. *A*: movement-related VP neuron time-locked to song. Same neuron as in Fig. 3*A top* to *bottom*: song spectrogram, neural signal, rasters, and rate histogram aligned to song. Pink shades indicate movements during singing. Scale bar for neural activity is 0.25 mV. *B*: same as *A* for the VTA neuron in Fig. 3*B*. *C*: scatterplot of intermotif cross correlation and difference in movement index between nonsinging and singing states. Each dot is a movement-related neuron ($N = 103$). Filled circles are neurons with significant song-locked activity ($N = 71$ neurons, $P < 0.05$, METHODS). Horizontal dashed line indicates threshold for song timing neurons (IMCC > 0.3). *D*: example neural activity at transitions from nonsinging to singing, same neuron as *A*. *Top* to *bottom*: song spectrogram, band-passed rectified accelerometer signal, neural signal, and rasters, aligned to onset of singing bouts. Blue and red lines indicate movement onsets outside and during singing. Blue shades in raster indicate movements outside song, with darker blue for the last movement before bout onset. Pink shades indicate movements during singing. Raster sorted by the timing of the last movement before song. *E*: same as *D*, but for transitions from singing to nonsinging. Raster sorted by timing of first movement after song. *F*, *top*: *Z* scored firing rate of neuron in *D* and *E*, aligned to movements immediately before (*left*) and after song (*right*). *Bottom*: same as *top*, for first and last movements during song. Blue/red bars indicate movement onsets outside/during song. Horizontal bars indicate significant response ($P < 0.05$, *Z* test, METHODS). cc, Correlation coefficient; VP, ventral pallidum; VTA, ventral tegmental area.

during singing. In addition, neurons that were precisely time-locked to movements during nonsinging became instead time-locked to song syllables (and not to body movements) during singing. These changes in tuning to distinct behavior modules could occur within tens of milliseconds at state boundaries. Although basal ganglia and cerebellar neurons are known to be able to be differentially tuned to internally versus externally (e.g., cue-driven) movements (21, 22), to our knowledge such dramatic and rapid change in limbic tuning to movement across behavioral states has never been reported.

Although the functional role of these state-dependent movement representations is unclear, one possibility is that the context-dependent switch of representations between movement timing and song timing may reflect a common underlying algorithm that evaluates the quality of *any* motor program currently being produced, for example, hop/orienting movements during nonsinging and syringeal movements during song. In this scenario, an outcome-weighted timing signal (such as a dopaminergic performance error signal) could be used to compute the predicted quality of ongoing performance, independent of the modality of the motor program. Although this hypothetical evaluation signal of two modalities of movements has not yet been measured simultaneously, the context-dependent movement selectivity observed in song error neurons is consistent with this idea.

Still, the switching of representation presents a puzzle for downstream neurons. Consider a neuron receiving input from song timing related neurons during singing. It can reliably decode the time of song. However, as soon as singing stops, this same recipient neuron should also switch its decoding algorithm (for example, by becoming inactive during nonsinging state), for the incoming signal has changed. If this is the case, another input indicating the state change (for example, by supplying an excitatory input only during singing) will be required. Although the possible source of this proposed gating signal remains to be found, we note that previously discovered "SongOn" and "SongOff" neurons

in VP (cf. Fig. 4 in Ref. 9), which turn on or off their activity during singing, act exactly like an "isSinging" gate. The potential local connections between these cell types within VP is unknown.

One caveat in our study is that we were unable to fully distinguish between types of movements—e.g., hopping versus neck rotations. Instead, we have measured acceleration at the level of the head and computed onset and offset timing of movements. Although birds appear to move in similar ways during singing and nonsinging periods (23), it's possible that there are subtle systematic differences between ostensibly similar movements when performed during singing and nonsinging. Future work with high-speed video will be required to test this possibility. Notwithstanding, the cessation of reliable time-locked firing to movements during singing was striking.

In new analyses for the present paper, we discovered that nonerror encoding VTA neurons (termed "VTAother" in Ref. 10) could exhibit precise song-locked discharge (Figs. 2*C* and 4*B*). Because error signals in the Area X-projecting VTA neurons are temporally precise, timing signals in VTA could play a role in shaping dopaminergic signals important for song learning.

In past work recording neural activity in VP and VTA from mammals, neurons have been categorized on the basis of their discharge patterns in relation to movement, reward, and/or reward prediction (4–6, 24–26). Our finding that VP and VTA neurons can exhibit tuning that depends on precisely what an animal is doing raises the possibility that neurons which fail to exhibit movement-locking in a chosen task may be movement-locked in others. More broadly, future studies may reveal that as an animal performs more tasks during VP and VTA recordings, more diverse classes of representation will be observed, even in single neurons.

GRANTS

This work was supported by a Simons Collaboration on the Global Brain Postdoctoral Fellowship and an NIH/National Institute of Neurological Disorders and Stroke (NINDS) Pathway to Independence (K99NS102520) award (V.G.), an NIH/NINDS Grant F32NS098634 (P.A.P.), an NIH/NINDS Grant R01NS094667, the Pew Charitable Trust, and the Klingenstein Neuroscience Foundations (J.H.G).

DISCLOSURES

No conflicts of interest, financial or otherwise, are declared by the authors.

AUTHOR CONTRIBUTIONS

R.C., V.G., A.C.R., P.A.P., and J.H.G. conceived and designed research; R.C., V.G., A.C.R., and P.A.P. performed experiments; R.C., V.G., A.C.R., P.A.P., and J.H.G. analyzed data; R.C., V.G., A.C.R., P.A.P., and J.H.G. interpreted results of experiments; R.C. prepared figures; R.C. and J.H.G. drafted manuscript; R.C. and J.H.G. edited and revised manuscript; R.C., V.G., A.C.R., P.A.P., and J.H.G. approved final version of manuscript.

REFERENCES

1. **Ahn S**, **Phillips AG.** Dopaminergic correlates of sensory-specific satiety in the medial prefrontal cortex and nucleus accumbens of the rat. *J Neurosci* 19: RC29, 1999. doi:10.1523/JNEUROSCI.19-19-j0003.1999.
2. **Papageorgiou GK**, **Baudonnat M**, **Cucca F**, **Walton ME.** Mesolimbic dopamine encodes prediction errors in a state-dependent manner. *Cell Rep* 15: 221–228, 2016. doi:10.1016/j.celrep.2016.03.031.
3. **Brooks VB.** How does the limbic system assist motor learning? A limbic comparator hypothesis. *Brain Behav Evol* 29: 29–53, 1986. doi:10.1159/000118670.
4. **Barter JW**, **Li S**, **Lu D**, **Bartholomew RA**, **Rossi MA**, **Shoemaker CT**, **Salas-Meza D**, **Gaidis E**, **Yin HH.** Beyond reward prediction errors: the role of dopamine in movement kinematics. *Front Integr Neurosci* 9: 39, 2015. doi:10.3389/fnint.2015.00039.
5. **Jin X**, **Costa RM.** Start/stop signals emerge in nigrostriatal circuits during sequence learning. *Nature* 466: 457–462, 2010. doi:10.1038/nature09263.
6. **Engelhard B**, **Finkelstein J**, **Cox J**, **Fleming W**, **Jang HJ**, **Ornelas S**, **Koay SA**, **Thiberge SY**, **Daw ND**, **Tank DW.** Specialized coding of sensory, motor and cognitive variables in VTA dopamine neurons. *Nature* 570: 509–513, 2019. doi:10.1038/s41586-019-1261-9.
7. **Eckmeier D**, **Geurten BR**, **Kress D**, **Mertes M**, **Kern R**, **Egelhaaf M**, **Bischof H-J.** Gaze strategy in the free flying zebra finch (*Taeniopygia guttata*). *PLoS One* 3: e3956, 2008. doi:10.1371/journal.pone.0003956.
8. **Williams H.** Choreography of song, dance and beak movements in the zebra finch (*Taeniopygia guttata*). *J Exp Biol* 204: 3497–3506, 2001. doi:10.1242/jeb.204.20.3497.
9. **Chen R**, **Puzerey PA**, **Roeser AC**, **Riccelli TE**, **Podury A**, **Maher K**, **Farhang AR**, **Goldberg JH.** Songbird ventral pallidum sends diverse performance error signals to dopaminergic midbrain. *Neuron* 103: 266–276.e4, 2019. doi:10.1016/j.neuron.2019.04.038.
10. **Gadagkar V**, **Puzerey PA**, **Chen R**, **Baird-Daniel E**, **Farhang AR**, **Goldberg JH.** Dopamine neurons encode performance error in singing birds. *Science* 354: 1278–1282, 2016. doi:10.1126/science.aah6837.
11. **Hisey E**, **Kearney MG**, **Mooney R.** A common neural circuit mechanism for internally guided and externally reinforced forms of motor learning. *Nat Neurosci* 21: 589–597, 2018. doi:10.1038/s41593-018-0092-6.
12. **Kearney MG**, **Warren TL**, **Hisey E**, **Qi J**, **Mooney R.** Discrete evaluative and premotor circuits enable vocal learning in songbirds. *Neuron* 104: 559–575.e6, 2019. doi:10.1016/j.neuron.2019.07.025.
13. **Xiao L**, **Chattree G**, **Oscos FG**, **Cao M**, **Wanat MJ**, **Roberts TF.** A basal ganglia circuit sufficient to guide birdsong learning. *Neuron* 98: 208–221.e5, 2018. doi:10.1016/j.neuron.2018.02.020.
14. **Humphries MD**, **Prescott TJ.** The ventral basal ganglia, a selection mechanism at the crossroads of space, strategy, and reward. *Prog Neurobiol* 90: 385–417, 2010. doi:10.1016/j.pneurobio.2009.11.003.
15. **Goldberg JH**, **Fee MS.** Singing-related neural activity distinguishes four classes of putative striatal neurons in the songbird basal ganglia. *J Neurophysiol* 103: 2002–2014, 2010. doi:10.1152/jn.01038.2009.
16. **Goldberg JH**, **Adler A**, **Bergman H**, **Fee MS.** Singing-related neural activity distinguishes two putative pallidal cell types in the songbird basal ganglia: comparison to the primate internal and external pallidal segments. *J Neurosci* 30: 7088–7098, 2010. doi:10.1523/JNEUROSCI.0168-10.2010.
17. **Tumer EC**, **Brainard MS.** Performance variability enables adaptive plasticity of 'crystallized' adult birdsong. *Nature* 450: 1240–1244, 2007. doi:10.1038/nature06390.
18. **Andalman AS**, **Fee MS.** A basal ganglia-forebrain circuit in the songbird biases motor output to avoid vocal errors. *Proc Natl Acad Sci USA* 106: 12518–12523, 2009. doi:10.1073/pnas.0903214106.
19. **Olveczky BP**, **Andalman AS**, **Fee MS.** Vocal experimentation in the juvenile songbird requires a basal ganglia circuit. *PLoS Biol* 3: e153, 2005. doi:10.1371/journal.pbio.0030153.
20. **Kao MH**, **Wright BD**, **Doupe AJ.** Neurons in a forebrain nucleus required for vocal plasticity rapidly switch between precise firing and variable bursting depending on social context. *J Neurosci* 28: 13232–13247, 2008. doi:10.1523/JNEUROSCI.2250-08.2008.
21. **Van Donkelaar P**, **Stein J**, **Passingham R**, **Miall R.** Neuronal activity in the primate motor thalamus during visually triggered and internally generated limb movements. *J Neurophysiol* 82: 934–945, 1999. doi:10.1152/jn.1999.82.2.934.
22. **Strick P**, **Hoover J**, **Mushiake H.** Role of the cerebellum and basal ganglia in voluntary movement (Proceedings of the 8th Tokyo

Metropolitan Institute for Neuroscience [TMIN] International Symposium [20th Anniversary of TMIN], Tokyo, 17–19 November 1992). *Neurology* 44: 2219–2219-a, 1993. doi:10.1212/WNL.44.11.2219-a.

23. **Yuan RC**, **Bottjer SW.** Multidimensional tuning in motor cortical neurons during active behavior. *eNeuro* 7: ENEURO.0109-20.2020, 2020. doi:10.1523/ENEURO.0109-20.2020.
24. **Tindell AJ**, **Berridge KC**, **Zhang J**, **Pecina S**, **Aldridge JW.** Ventral pallidal neurons code incentive motivation: amplification by mesolimbic sensitization and amphetamine. *Eur J Neurosci* 22: 2617–2634, 2005. doi:10.1111/j.1460-9568.2005.04411.x.
25. **Kaplan A**, **Mizrahi-Kliger AD**, **Israel Z**, **Adler A**, **Bergman H.** Dissociable roles of ventral pallidum neurons in the basal ganglia reinforcement learning network. *Nat Neurosci* 23: 556–559, 2020. doi:10.1038/s41593-020-0605-y.
26. **Richard JM**, **Stout N**, **Acs D**, **Janak PH.** Ventral pallidal encoding of reward-seeking behavior depends on the underlying associative structure. *eLife* 7: e33107, 2018. doi:10.7554/eLife.33107.